Silicon network structure and ^{29}Si spin-lattice relaxation in amorphous hydrogenated silicon

Man Ken Cheung and Mark A. Petrich
Department of Chemical Engineering, The Robert R. McCormick School of Engineering and Applied Science, Northwestern University, Evanston, Illinois 60208-3120
(Received 1 July 1991)

We report a NMR study of amorphous hydrogenated silicon (*a*-Si:H) that measures the ^{29}Si spin-lattice relaxation time T_1. Measurements of ^{29}Si T_1 are useful in learning about the silicon network structure and the localized states within the mobility gap. Coupling to paramagnetic dangling bonds is the predominant ^{29}Si spin-lattice relaxation mechanism in *a*-Si:H. Spin flipping of paramagnetic electrons, caused by coupling to the lattice, produces fluctuating local fields that stimulate nuclear spin-lattice relaxation. By comparing our experimental results with existing theory, we find that dangling bonds are randomly distributed in device-quality materials but are inhomogeneously distributed in non-device-quality materials. We also find that there are two simultaneously occurring dangling-bond spin-lattice relaxation mechanisms: one through the spin-orbit coupling modulated by thermal excitation of "two-level systems," and the other through hopping conduction between localized states near the Fermi level. Simple chemical-shift measurements are also helpful in characterizing *a*-Si:H. We find that the ^{29}Si resonance shifts upfield with increasing microstructure in the material.

I. INTRODUCTION

Remarkable advances in amorphous silicon (*a*-Si:H) technology were made during the past two decades. In the early 1970s, researchers at Standard Telephone Laboratories and the University of Dundee in the U.K. discovered that *a*-Si:H deposited by glow-discharge decomposition of silane had a lower density of localized states and higher electronic quality than sputtered or evaporated films.[1] Early work in the field focused predominantly on electronic characterization and overlooked almost completely the importance of structural and chemical characterization. It was only in the mid 1970s that widespread efforts to structurally and chemically characterize the material gave rise to the understanding that films that are suitable for device applications have a hydrogen content of approximately 10 at. % and are macroscopically homogeneous.[1] Hydrogen was presumed to play the role of passivating the dangling-bond defects. However, this explanation is not sufficient to account completely for the role of hydrogen because it is found that some ten to hundred times more hydrogen is incorporated into device-quality *a*-Si:H than is needed to passivate all the dangling bonds in unhydrogenated amorphous silicon (*a*-Si) as measured by electron paramagnetic resonance (EPR).[1]

In the 1980s, structural and chemical characterization yielded valuable information about the hydrogen microstructure in *a*-Si:H. Hydrogen is distributed inhomogeneously into two phases: a randomly isolated and a heavily clustered phase.[2,3] Subsequent nuclear magnetic resonance (NMR) and small angle x-ray scattering (SAXS) studies revealed that in device-quality *a*-Si:H each cluster consists of approximately 5–8 hydrogen atoms that are covalently bonded to silicon on internal surfaces of microvoids.[4,5]

NMR measurements of the temperature variation of ^{1}H spin-lattice relaxation time, T_1(H), showed a minimum near 40 K.[3] The cause of this behavior was initially ascribed to disorder modes or "two-level systems" (TLS's) which are commonly found in glasses and amorphous solids.[6,7] The presence of TLS's in *a*-Si:H has been deduced from low-frequency Raman scattering experiments and from the anomalous thermal properties of *a*-Si:H at low temperatures (0.1–5 K).[8,9] The presence of TLS's is not surprising, given the fact that the atomic arrangement in *a*-Si:H is not periodic. The network disorder in *a*-Si:H allows atoms to be bonded in configurations with different local minima of the potential energy, separated by a distribution of potential barriers.[10] However, theoretical calculations show that about 10% of the bonded hydrogen must be associated with these disorder modes in order to account for the experimental values of T_1(H).[11] This means that the hydrogen-associated TLS's, which actually exist in *a*-Si:H, are insufficient to account for the magnitude of T_1(H).[12]

It was later proposed that trapped hydrogen molecules in microvoids are the spin-lattice relaxation centers for ^{1}H in *a*-Si:H. In this model, the bonded hydrogen atoms relax by spin diffusion to these centers where the hydrogen atoms of an ortho-H_2 molecule (para-H_2 has zero nuclear spin) are relaxed rapidly by modulation of their dipole-dipole interaction via rotational motion of the molecule.[13] The presence of hydrogen molecules in *a*-Si:H is confirmed by the detection of an ortho-para conversion at 4.2 K,[14] and by direct observation of a Pake doublet from solid hydrogen in ^{1}H NMR spectra at temperatures below 10 K.[15] Deuteron magnetic resonance revealed also that deuterium molecules are present in *a*-Si:(D,H) samples and are responsible for deuteron spin-lattice relaxation.[16,17]

Observation of the silicon lattice in *a*-Si:H by NMR was discouraging at first because of the long ^{29}Si spin-lattice relaxation time. Therefore, there are no published

^{29}Si NMR spectra of *a*-Si:H, as far as we are aware of, which are obtained by direct excitation of the ^{29}Si nuclei. Cross-polarization with magic-angle (sample) spinning (CP-MAS) has been useful in the study of the silicon network structure in *a*-Si:H. The motivation for using CP-MAS was that silicon spectra could be obtained quickly, and it was hoped that these spectra would consist of many resolved chemical shifts representing the different bonding configurations. Unfortunately, a single broad line was observed in all these spectra. The residual linewidth of a CP-MAS ^{29}Si spectrum was very large, ranging from 50 to 60 ppm ($\sim$1 kHz).[18,19] The silicon line shape was independent of contact time, suggesting that the majority of the line broadening was due to intrinsic disorder in the *a*-Si:H network.[18] This conclusion is supported by a comparable linewidth calculated by a charge-density variation model.[19] Even though CP-MAS is a powerful technique, it is not quantitative because it uses the heteronuclear dipolar interaction to transfer energy from an abundant spin system (^{1}H) to a rare spin system (^{29}Si). Only ^{29}Si spins coupled with ^{1}H spins are observed, and the enhancement of signal intensity depends on the distance between a ^{29}Si spin and a ^{1}H spin.

The present work is an NMR study of *a*-Si:H that measures the ^{29}Si spin-lattice relaxation time T_1. Using standard NMR methods, we show that spin-lattice relaxation via paramagnetic centers is the dominant ^{29}Si relaxation mechanism in *a*-Si:H. Measurements of ^{29}Si T_1 provide useful information about the silicon network structure and the localized states within the mobility gap.

In Sec. II we will explain how we may control the effect of Hamiltonians on the time development of the macroscopic magnetization. In Sec. III we will review the theory of spin-lattice relaxation via paramagnetic centers to obtain a correlation between ^{29}Si T_1 and paramagnetic dangling-bond spin-lattice relaxation time T_{1S}. In Sec. IV we will describe the experimental details, and in Sec. V we will present our results and discussion.

II. NUCLEAR SPIN-LATTICE RELAXATION MECHANISM

The Hamiltonian describing the ^{29}Si spin system of undoped *a*-Si:H in the dark is the sum of a number of terms:[20]

$$\mathcal{H}=\mathcal{H}_Z+\mathcal{H}_{D,ii}+\mathcal{H}_{D,ij}+\mathcal{H}_{CS}+\mathcal{H}_{D,is} , \tag{1}$$

where $\mathcal{H}_Z=$ a Zeeman term representing the interaction between the observed nucleus (^{29}Si) and an external static magnetic field $B_0\hat{\mathbf{z}}$; $\mathcal{H}_{D,ii}=$ a homonuclear dipolar term representing the direct dipole-dipole interaction between ^{29}Si and ^{29}Si; $\mathcal{H}_{D,ij}=$ a dipolar term representing the direct dipole-dipole interaction between ^{29}Si and ^{1}H; $\mathcal{H}_{CS}=$ a chemical-shift term representing the interaction between the observed nucleus and nearby chemical bonding electrons; $\mathcal{H}_{D,is}=$ an electron-nucleus dipolar term representing the dipole-dipole interaction between ^{29}Si and a paramagnetic center.

The Zeeman part of the Hamiltonian is the dominant term, and the other components of the Hamiltonian are treated as perturbations. Since the perturbations convey most of the desired information about the spin system, they are normally studied by adopting a reference frame that eliminates the Zeeman term.[20] The transformation

$$\mathcal{H}^*=R_{z'}^{-1}(\omega_r t)R_y^{-1}(\theta)R_z^{-1}(\omega_z t)\mathcal{H}R_z(\omega_z t) \times R_y(\theta)R_{z'}(\omega_r t) \tag{2}$$

transforms the Hamiltonian of the spin system to a new reference frame.[21] $R_z(\omega_z t)$ is the rotation matrix describing the rotation about the z axis at frequency ω_z. $R_y(\theta)$ is the rotation matrix describing the rotation about the y axis, which transforms the coordinate system with z along the external field B_0 into a new coordinate system with z' inclined at an angle θ to z. $R_{z'}(\omega_r t)$ describes the rotation about z', which is the axis of physical rotation at frequency ω_r. Equation (1) becomes

$$\mathcal{H}^*=\hbar\omega_{\text{eff}}I_z+\frac{\gamma_i^2\hbar^2}{r_{12}^3}\left[\frac{(1-3\cos^2\theta)}{2}(\mathbf{I}_1\cdot\mathbf{I}_2-3I_{z1}I_{z2})+\cdots\right]+\frac{\gamma_i\gamma_j\hbar^2}{r_{ij}^3}\left[\frac{(1-3\cos^2\theta)}{2}(\mathbf{I}_i\cdot\mathbf{I}_j-3I_{zi}I_{zj})+\cdots\right]$$
$$+\gamma_i\hbar I_z\left[\sigma_{\text{iso}}+\frac{(1-3\cos^2\theta)}{2}\frac{\Delta\sigma}{2}+\cdots\right]B_0+\frac{\gamma_i\gamma_s\hbar^2}{r_{is}^3}(A_{is}+B_{is}+C_{is}+D_{is}+E_{is}+F_{is}) . \tag{3}$$

Here $\omega_{\text{eff}}=\omega_z-\omega_{0I}$, and when the angular frequency ω_z equals the Larmor frequency of the observed ^{29}Si nucleus ω_{0I}, the system is said to have been transformed to the "rotating frame," and the Zeeman part of the Hamiltonian is eliminated. γ_s and γ_i are the gyromagnetic ratios of the paramagnetic center and the nucleus, respectively. $\hbar$ is Planck's constant divided by 2π. r is the distance between two interacting dipoles. σ_{iso} is the isotropic chemical shift, and $\Delta\sigma$ is the chemical-shift anisotropy. The next three components of the Hamiltonian are the homonuclear dipolar, the heteronuclear dipolar, and the chemical-shift terms. We show the factor $(1-3\cos^2\theta)$ explicitly in these three terms to emphasize that when θ, the angle at which the sample rotation axis combined with the external static field $B_0\hat{\mathbf{z}}$ equals 54.74° (the "magic angle"), these three terms are suppressed if ω_r, the sample rotation frequency, is larger than the linewidth due to these interactions. We refrain from writing $(1-3\cos^2\theta)$ in the electron-nucleus dipolar term because magic-angle spinning is unable to suppress this interaction because the electron dipole moment is very large.[21,22] The linewidths due to ^{29}Si-^{29}Si dipolar coupling and chemical-shift anisotropy are at most 2 to 3 kHz; therefore, at the sample spin rates that we used (4.4–4.8 kHz),

these two interactions were eliminated. The linewidth contribution from ^{29}Si-^{1}H dipolar coupling is estimated to be 8 kHz for ^{29}Si bonded directly to ^{1}H, and it decreases to only 800 Hz for the next nearest neighbor. If all the hydrogen atoms are bonded to silicon as monohydrides, and if the concentration of hydrogen is 10 at. % merely 10% of the observed ^{29}Si nuclei are bonded directly to hydrogen and are not completely decoupled from the hydrogen at sample spin rates of 4.4–4.8 kHz. NMR experiments with and without high-power proton decoupling on our samples showed negligible ^{29}Si-^{1}H dipolar contribution to the linewidths. Hence, under magic-angle spinning conditions at rates of 4.4–4.8 kHz, the Hamiltonian of a ^{29}Si nucleus is approximately

$$\mathcal{H}^* \approx \gamma_i \hbar I_z \sigma_{\rm iso} B_0 + \frac{\gamma_i \gamma_s \hbar^2}{r_{is}^3}(A_{is}+B_{is}+C_{is}+D_{is}+E_{is}+F_{is}) , \quad (4)$$

where

$$A_{is} = I_z S_z (1-3\cos^2\theta_{is}), \quad \Delta m_i = \Delta m_s = 0 ;$$

$$B_{is} = -\tfrac{1}{4}(I^+S^- + I^-S^+)(1-3\cos^2\theta_{is}) , \quad \Delta(m_i+m_s)=0 ;$$

$$C_{is} = -\tfrac{3}{2}(I^+S_z + I_z S^+)\sin\theta_{is}\cos\theta_{is}e^{-i\phi} , \quad \Delta(m_i+m_s)=1 ;$$

$$D_{is} = -\tfrac{3}{2}(I^-S_z + I_z S^-)\sin\theta_{is}\cos\theta_{is}e^{i\phi} , \quad \Delta(m_i+m_s)=-1 ;$$

$$E_{is} = -\tfrac{3}{4}I^+S^+\sin^2\theta_{is}e^{-2i\phi}, \quad \Delta(m_i+m_s)=2 ;$$

$$F_{is} = -\tfrac{3}{4}I^-S^-\sin^2\theta_{is}e^{2i\phi}, \quad \Delta(m_i+m_s)=-2 ;$$

I_z and S_z are the z components of the angular momentum operators for ^{29}Si and the electron, respectively. I^+ (S^+) and I^- (S^-) are, respectively, the raising and lowering operators for ^{29}Si (electron). θ_{is} is the angle that the line joining the nucleus and the paramagnetic center makes with the static magnetic field $B_0\hat{z}$.

A ^{29}Si nucleus in the upper Zeeman energy level can make a transition to the lower Zeeman energy level by releasing energy to the surrounding lattice. This process returns the ^{29}Si spin system to the thermal equilibrium ground state. The rate of return to thermal equilibrium is characterized by the spin-lattice relaxation time T_1. In order to relax, a ^{29}Si nucleus must come under the influence of randomly fluctuating magnetic fields near its Larmor frequency. Such fluctuating fields can arise from coupling to mobile carriers, molecular motions, or dipole moments.[23,24]

We have neglected the coupling between mobile carriers and ^{29}Si nuclei in arriving at Eq. (4) because we are considering only undoped a-Si:H samples in the dark. The dark conductivity of undoped a-Si:H is on the order of 10^{-8} to 10^{-12} $(\Omega\,\text{cm})^{-1}$, which translates into a mobile carrier density ranging from 10^5 to 10^9 cm^{-3}, if we assume that the mobility in the extended states is 10 cm^2 s^{-1} V^{-1}.[25] The mobile carrier density is far smaller than the paramagnetic center density (10^{15} to 10^{18} cm^{-3}) found in our undoped a-Si:H samples. Therefore, it is most unlikely that mobile carriers can make a significant contribution to the ^{29}Si spin-lattice relaxation rate in the present investigation.

^{29}Si spin-lattice relaxation through the chemical-shift anisotropy is an important mechanism only when large amplitude molecular motions are present.[23,24,26] This is not the case in a-Si:H because the silicon network is a rigid three-dimensional structure, and rapid molecular motions are not present.

We have already argued that the electron-nucleus dipolar coupling is the strongest of all the different dipolar couplings present in a-Si:H. Hence, the remaining candidate for the most dominant relaxation mechanism in a-Si:H is relaxation via paramagnetic centers.

The flipping of an electronic spin caused by coupling to the lattice produces a fluctuating local field which, in turn, stimulates spin-lattice relaxation of the surrounding nuclei. The terms B_{is}, C_{is}, D_{is}, E_{is}, and F_{is} in Eq. (4), combined with the time variation of the electron spin states, provide a nuclear spin-lattice relaxation mechanism.[24,27,28] For NMR transitions such as $\Delta m_i = -1$, the contribution to the relaxation time T_{1I} for a nuclear spin using the terms B_{is}, D_{is}, and F_{is} is given by[28]

$$\frac{1}{2T_{1I}} = \frac{1}{16}\frac{\gamma_i^2}{r_{is}^6}(1-3\cos^2\theta_{is})^2 J_0(\omega) + \frac{9}{4}\frac{\gamma_i^2}{r_{is}^6}\sin^2\theta_{is}\cos^2\theta_{is}J_1(\omega) + \frac{9}{16}\frac{\gamma_i^2}{r_{is}^6}\sin^4\theta_{is}J_2(\omega) . \quad (5)$$

$J_0(\omega)$, $J_1(\omega)$, and $J_2(\omega)$ are the spectral densities of the Fourier spectrum of the expectation values of the components of the electron magnetic moment. These three spectral densities correspond to transitions in which there are no net spin flips, one spin flip, and two spin flips. If the probability of the electron not undergoing transition for a time t is assumed to decay exponentially with a time constant τ_c, the spectral densities are given by[27]

$$J_0(\omega) = J_0(\omega_{0I}-\omega_{0s}) = 2\gamma_s^2\hbar^2 S(S+1)\frac{\tau_c}{1+(\omega_{0I}-\omega_{0S})^2\tau_c^2} , \quad (6a)$$

$$J_1(\omega) = J_1(\omega_{0I}) = \tfrac{2}{3}\gamma_s^2\hbar^2 S(S+1)\frac{\tau_c}{1+(\omega_{0I})^2\tau_c^2} , \quad (6b)$$

$$J_2(\omega) = J_2(\omega_{0I}+\omega_{0S}) = \tfrac{4}{3}\gamma_s^2\hbar^2 S(S+1)\frac{\tau_c}{1+(\omega_{0I}+\omega_{0S})^2\tau_c^2} . \quad (6c)$$

S is the electronic spin quantum number ($S=\frac{1}{2}$). ω_{0I} is the Larmor frequency of ^{29}Si, and ω_{0S} is the Larmor frequency of the electron.

The expressions for transitions with $\Delta m_i = +1$ are the same except that the spectral densities are taken at nega-

tive frequencies in the Fourier spectrum.[28]

Averaging over the angle θ_{is} [$\langle(1-3\cos^2\theta_{is})^2\rangle=\frac{4}{5}$, $\langle\sin^2\theta_{is}\cos^2\theta_{is}\rangle=\frac{2}{15}$, $\langle\sin^4\theta_{is}\rangle=\frac{8}{15}$], the spin-lattice relaxation time T_{1I} of a ^{29}Si nucleus is expressed as[23]

$$\frac{1}{T_{1I}}=\frac{2}{5}\frac{\gamma_I^2\gamma_S^2\hbar^2}{r_{is}^6}S(S+1)\left[\frac{1}{3}\frac{\tau_c}{1+(\omega_{0I}-\omega_{0S})^2\tau_c^2}+\frac{\tau_c}{1+\omega_{0I}^2\tau_c^2}+\frac{2\tau_c}{1+(\omega_{0I}+\omega_{0S})^2\tau_c^2}\right]. \quad (7)$$

As ω_{0S} (10^{12} rad sec^{-1}) $\gg\omega_{0I}$ (10^8 rad sec^{-1}) and usually $\tau_c>10^{-8}$ sec rad^{-1}, only the second term contributes appreciably to the spin-lattice relaxation.[28] Thus,

$$\frac{1}{T_{1I}}\approx\frac{2}{5}\frac{\gamma_I^2\gamma_S^2\hbar^2}{r_{is}^6}S(S+1)\frac{\tau_c}{1+\omega_{0I}^2\tau_c^2}=\frac{C}{r_{is}^6}, \quad (8)$$

where now

$$C=\tfrac{2}{5}\gamma_I^2\gamma_S^2\hbar^2S(S+1)\frac{\tau_c}{1+\omega_{0I}^2\tau_c^2} \quad (9)$$

is independent of the position of the given nucleus but is dependent on the correlation time τ_c, which is related to the paramagnetic center spin-lattice relaxation time T_{1S} by the relation $2\pi\tau_c=T_{1S}$.[28]

III. THEORY OF SPIN-LATTICE RELAXATION VIA PARAMAGNETIC CENTERS

There are extensive theoretical studies of the problem of nuclear spin-lattice relaxation in solids due to dilute paramagnetic centers augmented by spin diffusion.[28–32] The coupling between the magnetic moment of the paramagnetic center and the magnetic moments of the nuclei is described by the dipolar Hamiltonian. The direct relaxation rate of a nucleus at a distance r_{is} from a single paramagnetic center is given by Eq. (8).

Let $m(t,\{|\mathbf{r}-\mathbf{r}_n|\})$ be the z component of the nuclear spin magnetization at time t and position $\mathbf{r}$. The rate of change of the nuclear spin magnetization in the absence of radio frequency excitation is given by the following diffusion equation:

$$\frac{\partial m(t,\{|\mathbf{r}-\mathbf{r}_n|\})}{\partial t}=D\nabla^2m(t,\{|\mathbf{r}-\mathbf{r}_n|\})-C[m(t,\{|\mathbf{r}-\mathbf{r}_n|\})-m_0]\times\sum_n|\mathbf{r}-\mathbf{r}_n|^{-6}, \quad (10)$$

where $\mathbf{r}_n$ is the location of a paramagnetic center, D is the spin diffusion coefficient, and m_0 is the thermal equilibrium value of $m(t,\{|\mathbf{r}-\mathbf{r}_n|\})$. The first term on the right side of the equation represents the rate of change of $m(t,\{|\mathbf{r}-\mathbf{r}_n|\})$ due to spin diffusion, and the second term represents the rate of change of $m(t,\{|\mathbf{r}-\mathbf{r}_n|\})$ due to direct relaxation by coupling to paramagnetic centers.

In the theory of nuclear spin-lattice relaxation via paramagnetic centers, there are several important characteristic length parameters: (i) the mean spacing between paramagnetic centers $R=[3/(4\pi N_p)]^{1/3}$, where N_p is the density of paramagnetic centers; (ii) the mean lattice constant, a; (iii) the diffusion barrier radius b; and (iv) the pseudo-potential radius $\beta=(C/D)^{1/4}$, where C is defined in Eq. (9), and D is the spin diffusion coefficient in Eq. (10). The diffusion barrier radius b can be defined as that distance from the paramagnetic center where the magnetic field due to the paramagnetic center equals the local dipolar field produced by nuclei. A nucleus within the diffusion barrier radius has a Larmor frequency much different from nuclei outside of the diffusion barrier radius. Thus, this nucleus is decoupled from the rest of the nuclei in the bulk, and it neither participates in the spin diffusion process, nor contributes to the nuclear resonance line. The pseudo-potential radius β is a measure of the competing contributions between direct relaxation and spin diffusion. In solving Eq. (10), three cases may be considered: no spin diffusion, diffusion limited, and direct relaxation limited (or rapid diffusion).

By using the single-paramagnetic-center model, which assumes that the sample can be covered by a set of randomly distributed spheres, each of which has only one paramagnetic center that is important in influencing the total nuclear spin-lattice relaxation in that sphere, the ensemble-average magnetization in the no-spin-diffusion case may be shown to be[33]

$$M(t)=M_0\left\{1-\exp\left[V_bN_p-\left[\frac{t}{T_1}\right]^{1/2}\right]\right\}. \quad (11)$$

M_0 is the thermal equilibrium magnetization, and V_b is the volume of the spherical region defined by the diffusion barrier radius. Nuclei within this region are not observable and do not participate in spin diffusion. If $V_bN_p\ll1$, then for short times $M(t)$ is proportional to $t^{1/2}$, which has been confirmed experimentally.[30]

In the diffusion-limited case, $M(t)$ is initially nonexponential, but approaches an exponential function at long times.[30] In the direct-relaxation-limited case, $M(t)$ is exponential at all times.[30] A dimensionless ratio

$$\delta=\frac{\beta^2}{2b^2} \quad (12)$$

serves as a criterion for distinguishing between the diffusion-limited and direct-relaxation-limited cases.[31] A sudden transition from the diffusion-limited to the direct-relaxation-limited case occurs near $\delta=1$.

In the diffusion-limited case $\delta\gg1$, the nuclear spin-lattice relaxation rate approaches[31,32]

$$\frac{1}{T_1}\approx\frac{8\pi}{3}N_pD\beta=\frac{8\pi}{3}N_pC^{1/4}D^{3/4}. \quad (13)$$

For the direct-relaxation-limited case $\delta\ll1$, the nuclear spin-lattice relaxation rate approaches[30–32]

$$\frac{1}{T_1}\approx\frac{8\pi}{3}N_pD\beta\frac{\beta^3}{2b^3}=\frac{4\pi}{3}N_pCb^{-3}. \quad (14)$$

The nuclear spin-lattice relaxation rate in the no-spin-diffusion case is approximately given by,[32]

$$\frac{1}{T_1} \approx \lambda_0 C N_p^2 + \lambda (CD)^{1/2} N_p^{4/3} ,$$

$$\text{where } \lambda_0 \approx 2 \text{ and } \lambda \approx 50 . \quad (15)$$

The diffusion barrier radius b can be approximated by[30]

$$b = \left[\frac{\gamma_s}{\gamma_i} \right]^{1/3} a, \quad \text{when } T_{1S} > T_2 \text{ or } \gamma_s \hbar B_0 > 2kT \quad (16a)$$

or

$$b = \left[\frac{\gamma_s^2 \hbar B_0}{\gamma_i 2kT} \right]^{1/3} a ,$$

$$\text{when } T_{1S} < T_2 \text{ and } \gamma_s \hbar B_0 < 2kT . \quad (16b)$$

T_2 is the nuclear spin-spin relaxation time, and kT is the lattice thermal energy. Generally in a-Si:H, $T_{1S}(=2\pi\tau_c) \ll T_2 \approx 1/(^{29}\text{Si}$ spectral linewidth), and $\tau_c > 10^{-8}$ sec rad^{-1}, so that $\omega_{0I}\tau_c \gg 1$.[34,35] At the temperatures and the magnetic field strength used in this study, $\gamma_s \hbar B_0 < 2kT$. Hence, the diffusion barrier radius is determined by Eq. (16b) and is proportional to $B_0^{1/3}$. C is defined in Eq. (9) and is proportional to $B_0^{-2} T_{1S}^{-1}$ because $\omega_{0I} = -\gamma_i B_0$ and $T_{1S} = 2\pi\tau_c$. We rewrite Eqs. (13) and (14) to show the power-law dependence of the nuclear spin-lattice relaxation time T_1 on the sample parameters. For the diffusion-limited case,

$$T_1 \propto N_p^{-1} D^{-3/4} B_0^{1/2} T_{1S}^{1/4} , \quad (17)$$

and for the direct-relaxation-limited case,

$$T_1 \propto N_p^{-1} B_0^3 T^{-1} T_{1S} . \quad (18)$$

IV. EXPERIMENT

The a-Si:H samples for the present study were prepared in a home-built stainless-steel parallel-electrode plasma-enhanced chemical vapor deposition reactor. The electrodes were 17.8 cm in diameter and were 3.5 cm apart. Substrates were placed on the grounded bottom electrode (anode), which was heated externally by a disk heater. The output of a rf signal generator was amplified and was then capacitively coupled through an impedance matching network to the upper electrode. Prior to each deposition, the reactor was evacuated to less than 5×10^{-5} Torr. The films were approximately 3 μm thick, as measured by a mechanical stylus. The deposition conditions are listed in Table I.

Samples for hydrogen concentration, EPR defect density, and ^{29}Si NMR measurements were deposited on thin aluminum foils. Films were removed from the foil substrates by dissolving the aluminum in dilute hydrochloric acid. The flakes were separated out by filtration, washed with distilled water, and dried overnight. The flakes were ground into powder. Samples for Fourier-transform infrared (FTIR) measurements were deposited on crystalline silicon wafers, and samples for optoelectronic property measurements were deposited on Corning 7059 glass.

Hydrogen concentrations were measured with a Perkin-Elmer 240 Elemental Analyzer. Paramagnetic defect densities were measured with a home-built X-band EPR spectrometer. DPPH (α,α'-diphenyl-β-picrylhydrazyl) served as the standard to calibrate signal intensity measurements. IR absorption spectra were obtained with a Mattson Alpha-Centauri FTIR spectrometer. The intensities of the 2080 cm^{-1} and 2000 cm^{-1} IR absorptions were calculated by a Gaussian curve fit program. Optical gap energies were measured with a Perkin-Elmer 330 UV/VIS/NIR spectrophotometer.

NMR measurements were carried out using a Varian VXR 300 spectrometer operating at a frequency of 59.59 MHz for the ^{29}Si resonance in a field of 7 T. Samples weighing about 150 mg were packed into 7-mm sapphire rotors. The samples were spun at a rate of 4.4–4.8 kHz at the magic angle, in a Doty Scientific variable-temperature solid-state NMR probe. Chemical-shift values are reported relative to tetramethylsilane (TMS). Tetrakis (trimethylsilyl)silane (Aldrich Chemical No. 32,992-4), used as an external reference, has two peaks at shift values -9.7 ppm and -135 ppm from TMS.[36]

^{29}Si spin-lattice relaxation (T_1) times were measured from 293 to 348 K using a progressive saturation (t-90°) pulse sequence.[37] For each t value, seven pulses were made, but the first three pulses were used to achieve steady state and thus not signal averaged. Because of the long ^{29}Si T_1 values (2–3 h), a single T_1 measurement took more than three days. We did not measure T_1 at temperatures higher than 348 K to minimize annealing effects during the course of a long NMR session. We did not measure T_1 at temperatures lower than 293 K because the T_1 will be even longer, and the measurement will become even more tedious.

V. RESULTS AND DISCUSSION

Based on photoconductivity, dark conductivity, and EPR data, films A and B are considered to be device-quality materials. The photoconductivity of film B is 1.4×10^{-4} $(\Omega\,\text{cm})^{-1}$, and the dark conductivity is 5.5×10^{-10} $(\Omega\,\text{cm})^{-1}$. After exposing film B to a light source of intensity 120 mW cm^{-2} for 30 min, the ratio of

TABLE I. Deposition conditions.

Sample	Silane flow rate (sccm)	Hydrogen flow rate (sccm)	Reactor pressure (mTorr)	Substrate temperature (°C)	Discharge power (W)	rf frequency (MHz)
A	50	0	200	240	10	13.56
B	50	0	200	180	10	27.12
C	50	50	700	50	10	13.56

TABLE II. Summary of results from various analytical methods showing the hydrogen concentration, the dangling-bond density, the amount of microstructure (derived from infrared absorption spectra), the ^{29}Si magic-angle spinning (MAS) NMR line-center position, and the ^{29}Si MAS NMR linewidth of *a*-Si:H.

	Elemental analyzer	EPR	FTIR	^{29}Si MAS NMR	
Sample	Hydrogen concentration	Dangling-bond density	Microstructure parameter R	Line-center position	FWHM
A	10.3 at. %	8.4×10^{14} cm^{-3}	0.135	-64 ± 3 ppm	54 ± 1 ppm
B	15.1 at. %	1.5×10^{15} cm^{-3}	0.599	-72 ± 3 ppm	56 ± 2 ppm
C	29.3 at. %	2.8×10^{17} cm^{-3}	0.970	-81 ± 3 ppm	57 ± 3 ppm

dark conductivities, after and prior to light exposure, is 9.5×10^{-2}. Film *C* is a poor quality material. It did not adhere well to either the aluminum or the crystalline silicon substrate and has a reddish color. The optical gap energies (E_{04}) for films *A* and *C* are 1.77 and 1.90 eV, respectively. Table II summarizes the results from hydrogen concentration, EPR defect density, FTIR, and NMR measurements. Table III lists ^{29}Si T_1 values at different temperatures. The estimated error in the T_1 values is 10%.

We are unable to use existing theory to predict nuclear spin-lattice relaxation times in the present work.[28–32] The main reasons are that the field dependence of the electron spin-lattice relaxation time T_{1S} and the value of the ^{29}Si spin-spin diffusion coefficient D in *a*-Si:H are still very much unknown. The literature values of T_{1S} are usually measured with *X*-band EPR at a field of about 3.3 kG,[34,35] but our NMR experiments were performed at a field of 70 kG. The field dependence of T_{1S} will change the relationship between the ^{29}Si T_1 and B_0. More EPR studies of *a*-Si:H are needed, and the T_{1S} measurements should cover a wider temperature range because the relation of T_{1S} with B_0 may change with temperature.

We show in Fig. 1 that the ^{29}Si MAS NMR line-center position is correlated to a microstructure parameter R, which is the ratio of the integrated density of the IR absorption centered at 2080 cm^{-1} to the sum of the integrated intensities of the IR absorptions centered at 2000 cm^{-1} and 2080 cm^{-1}.[38] The parameter R describes that fraction of hydrogen bonded in some sort of microstructure [microvoids and/or $(SiH_2)_n$]. Void fractions determined by flotation measurements[39] and small angle x-ray scattering[40] (SAXS) are found to increase with R, i.e., with the fraction of hydrogen contributing to the 2080 cm^{-1} absorption. The ^{29}Si MAS NMR line-center position is most likely an average value of the isotropic chemical shifts, reflecting the local bonding configurations.[41,42] ^{1}H NMR measurements of *a*-Si:H indicated that the concentration of hydrogen in the clustered phase increases linearly with the intensity of the 2080 cm^{-1} IR absorption.[4] The clustered phase hydrogens are covalently bonded to silicon on internal surfaces of microvoids.[4,5] Hence, the correlation in Fig. 1 can be interpreted as the upfield shifting from TMS of the ^{29}Si MAS NMR line-center position (shielding of ^{29}Si) with increasing clustering of hydrogens. This observation is consistent with the reported correlation of ^{29}Si CP-MAS line position with the line shape of the ^{1}H NMR spectrum.[41]

The full-width at half-maximum (FWHM) of a typical ^{29}Si spectrum of *a*-Si:H samples from our laboratory taken without MAS is about 100 ppm (6 kHz), but the linewidth of a typical ^{29}Si spectrum taken with MAS is about 60 ppm (3.6 kHz). The residual linewidth of the ^{29}Si MAS NMR spectrum is most probably due to chemical-shift dispersions, arising from disorder in the silicon network.[41,42] An attempt was made to establish an empirical correlation between the bond-angle distribution width and the ^{29}Si MAS NMR linewidth in unhydrogenated amorphous (*a*-Si).[42] However, when the correlation was applied to *a*-Si:H, the correlation predicted a linewidth that was 9 ppm larger than the observed value.[42] The lower value in *a*-Si:H could easily result from modifications of the local electronic environment of the ^{29}Si nuclei by the addition of hydrogen. Further theoretical study of *a*-Si:H will be helpful in clarifying the

TABLE III. Summary of variable-temperature ^{29}Si T_1 experiments on device-quality *a*-Si:H. At any given temperature, sample *B* has a faster spin-lattice relaxation than sample *A* because sample *B* has a higher dangling-bond density.

Sample *A*		Sample *B*	
Temperature (K)	T_1 (min)	Temperature (K)	T_1 (min)
298	138	293	78
313	113		
333	98		
341	92		
348	82	348	47

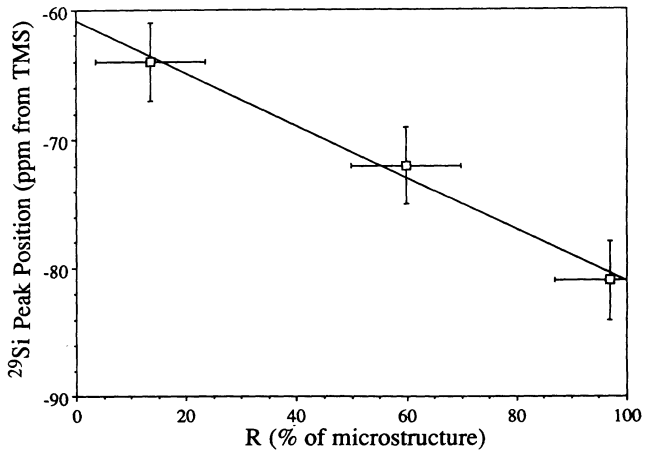

FIG. 1. ^{29}Si NMR line-center position vs amount of microstructure expressed by the R parameter, which is derived from infrared absorption data. ^{29}Si chemical shifts are sensitive to hydrogen-related microstructure in *a*-Si:H.

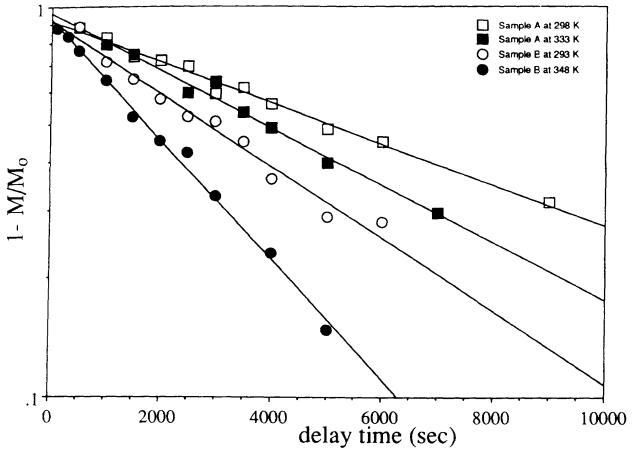

FIG. 2. Semilogarithmic plots of magnetization recovery vs delay time during ^{29}Si T_1 experiments on device-quality a-Si:H. The single exponential behavior observed is indicative of a direct-relaxation-limited T_1 process.

relationship between ^{29}Si MAS NMR linewidth and local silicon network disorder.

We have observed, within detection limits of our NMR spectrometer, that ^{29}Si spin-lattice relaxation in the two device-quality samples is a single exponential process for all times, as shown in the semilogarithmic plot of Fig. 2, suggesting that ^{29}Si spin-lattice relaxation in device-quality a-Si:H is direct-relaxation-limited.[30] At any given temperature, sample B has a faster spin-lattice relaxation than sample A because sample B has a higher paramagnetic center density.

The ^{29}Si spin-lattice relaxation in the non-device-quality sample C is not a single exponential process, as shown in Fig. 3, suggesting that relaxation is diffusion limited.[30,43] The departure from single exponential behavior suggests a distribution of spin-lattice relaxation times. The distribution of spin-lattice relaxation times can arise from an inhomogeneous distribution of paramagnetic centers because silicon-silicon spin diffusion is too slow to completely average out the differences in spin-lattice relaxation times due to the differences in distance between the ^{29}Si nuclei and the paramagnetic relaxation sites.[43] The data in Fig. 3 can be fitted by two exponential functions with T_1 values of 8 and 40 min:

$$1-\frac{M}{M_0}=\Phi^{\text{fast}}\exp\left[-\frac{t}{T_1^{\text{fast}}}\right]+\Phi^{\text{slow}}\exp\left[-\frac{t}{T_1^{\text{slow}}}\right], \quad (19)$$

where Φ^{fast} and Φ^{slow} are the fraction of ^{29}Si nuclei in the fast-relaxing phase and in the slow-relaxing phase, respectively. About 48% of the silicon atoms are in the fast-relaxing phase, which is likely to be regions with high-paramagnetic-center density.

We have measured ^{29}Si T_1 values of the two device-quality samples at temperatures ranging from 293 to 348 K. For a given device-quality sample at a constant Zeeman field, Eq. (18) shows that T_1 is proportional to $T^{-1}T_{1S}$, where T is the absolute temperature, and T_{1S} is the dangling-bond spin-lattice relaxation time. If T_{1S} is proportional to T^{-2}, as previously reported,[44] then T_1 is proportional to T^{-3}. In Fig. 4, assuming that only the power-law relationship exists, we plot $\ln T_1$ versus $\ln T$. This plot shows that T_1 is proportional to T^{-3}, confirming that T_{1S} is proportional to T^{-2}. T_{1S} relaxation is typically through the spin-orbit coupling modulated by thermal excitation of localized disorder modes or two-level systems (TLS's).[44,45]

We can also plot our T_1 data assuming that only a thermally activated relaxation mechanism exists, as

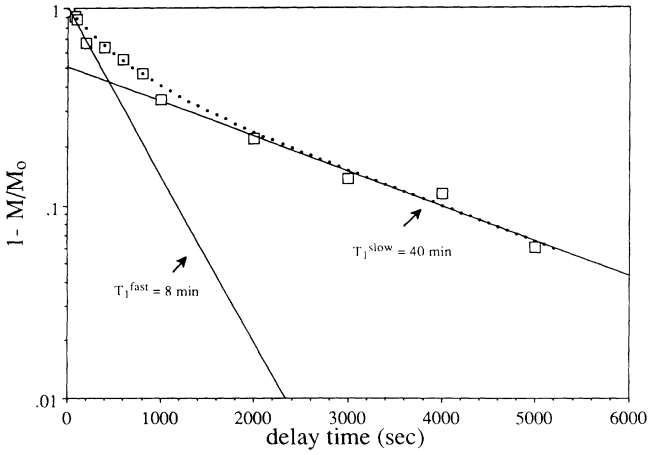

FIG. 3. Semilogarithmic plot of magnetization recovery vs delay time during a ^{29}Si T_1 experiment on non-device-quality a-Si:H. Data points are represented by open squares. The data is fitted well by the sum of two exponential functions with time constants of 8 and 40 min. These exponential functions are shown as solid lines on this plot. The dotted line is the sum of the two exponential functions. This data suggests that paramagnetic centers are inhomogeneously distributed in this sample.

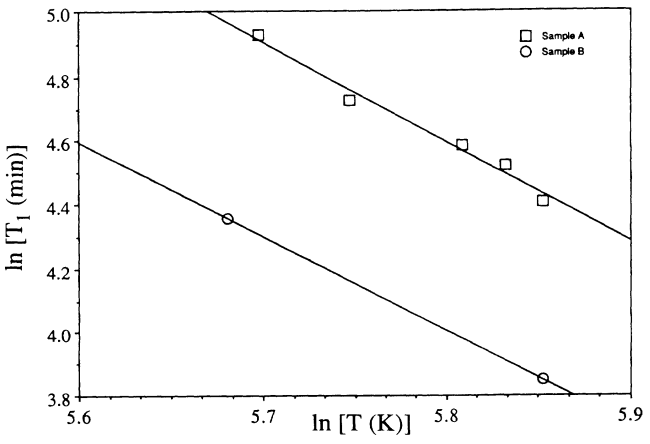

FIG. 4. Logarithm of ^{29}Si T_1 vs logarithm of T, the temperature during a ^{29}Si T_1 experiment on device-quality a-Si:H. The slope of these plots is -3, indicating that the electron spin-lattice relaxation time is proportional to T^{-2}. This behavior is typical of electron spin-lattice relaxation through spin-orbit coupling modulated by thermal excitation of localized disorder modes.

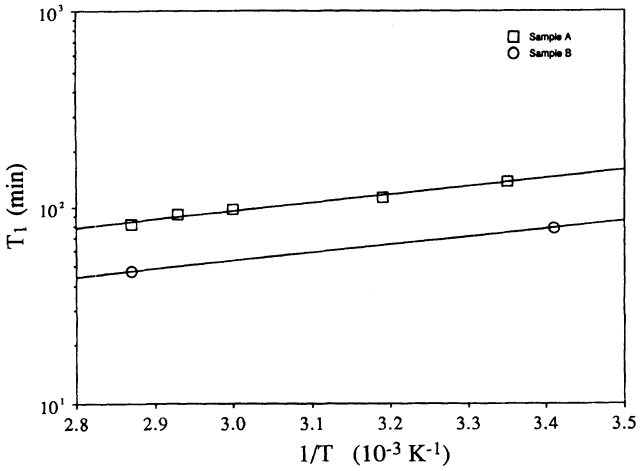

FIG. 5. Plot of ^{29}Si T_1 for device-quality a-Si:H vs inverse temperature. The slope of these plots indicates a relaxation activation energy of 0.08 eV.

shown in Fig. 5. The slope of the lines represents an activation energy ΔE of 0.08 eV. This value is calculated assuming that only the activated process exists and should be regarded as an upper limit. The magnitude is comparable to that for phonon-assisted hopping conduction between localized states near the Fermi level.[25] If the dangling-bond spin-lattice relaxation mechanism is a two-step phonon process (Orbach process), then T_{1S} is proportional to $\exp(\Delta E/kT)$.[46] The Orbach relaxation process involves phonon excitation of the paramagnetic center from the upper Zeeman level of the ground state to a nearby excited state, and subsequently deexcitation to the lower Zeeman level of the ground state. According to Eq. (18), in the small temperature range of 293 to 348 K, ^{29}Si T_1 is approximately proportional to $\exp(\Delta E/kT)$. Therefore, we observe a thermally activated T_1 behavior in Fig. 5. Variable-temperature NMR studies of a silicon crystal, with an estimated paramagnetic center density of 1.1×10^{16} cm^{-3}, have yielded an activation energy of a similar magnitude, 0.07 eV.[47] The room-temperature T_1 of the silicon crystal (290 min) is two to four times longer than those of our amorphous samples. The presence of TLS's as an extra set of structural excitations in our amorphous samples may account for the shorter ^{29}Si spin-lattice relaxation times.

It seems likely that there are two simultaneously occurring paramagnetic dangling-bond T_{1S} relaxation mechanisms in a-Si:H at the temperatures studied here. They can be represented by the rate equation:

$$\frac{1}{T_{1S}}=K'T^2+K''\exp\left[-\frac{\Delta E}{kT}\right],$$

where K' and K'' are constants . (20)

Since we observe a relatively small change in T_1 over a limited temperature range, it is not possible to distinguish clearly which mechanism is more important in our experiments. At temperatures from 5 to 300 K, the first term on the right side has been shown to dominate.[44] As temperatures rise well above room temperature, the number of phonons with high enough energy to activate hopping conduction increases, and the second term gains importance.

VI. CONCLUSIONS

We have demonstrated that coupling to paramagnetic dangling bonds is the predominant ^{29}Si spin-lattice relaxation mechanism in a-Si:H. Paramagnetic dangling bonds are randomly distributed throughout our device-quality samples, but are inhomogeneously distributed in our non-device-quality sample. Some regions in our non-device-quality sample are heavily clustered with dangling bonds. There are two simultaneously occurring dangling-bond spin-lattice relaxation mechanisms: one through the spin-orbit coupling modulated by thermal excitation of two-level systems and the other through hopping conduction between gap states. We have also found that the ^{29}Si MAS NMR line-center position shifts upfield from TMS with increasing hydrogen microstructure.

ACKNOWLEDGMENTS

The authors would like to thank Professor J. Kakalios and his group at the University of Minnesota for measuring the conductivities, and our colleague Hsueh Yi Lu for measuring the dangling-bond densities and providing the Gaussian curve fit program. We are also grateful to Clark Millikan and Scott Woehler for their hospitality when one of us (M.K.C.) worked at the Chemistry Department's NMR facility.

[1] J. C. Knights, in *The Physics of Hydrogenated Amorphous Silicon I*, edited by J. D. Joannopoulos and G. Lucovsky, Topics in Applied Physics Vol. 55 (Springer-Verlag, New York, 1984), pp. 5–62.
[2] J. A. Reimer, R. W. Vaughan, and J. C. Knights, Phys. Rev. B **24**, 3360 (1981).
[3] W. E. Carlos and P. C. Taylor, Phys. Rev. B **26**, 3605 (1982).
[4] K. K. Gleason, M. A. Petrich, and J. A. Reimer, Phys. Rev. B **36**, 3259 (1987).
[5] A. H. Mahan, D. L. Williamson, B. P. Nelson, and R. S. Crandall, Phys. Rev. B **40**, 12 024 (1989).
[6] W. E. Carlos and P. C. Taylor, Phys. Rev. Lett. **45**, 358 (1980).
[7] J. A. Reimer, R. W. Vaughan, and J. C. Knights, Phys. Rev. B **23**, 2567 (1981).
[8] S. A. Lyon and R. J. Nemanich, Physica B+C **117-118B**, 871 (1983).
[9] J. E. Graebner, B. Golding, L. D. Allen, J. C. Knights, and D. K. Biegelsen, Phys. Rev. B **29**, 3744 (1984).
[10] P. W. Anderson, B. I. Halperin, and C. M. Varma, Philos. Mag. **25**, 1 (1972).
[11] B. Movaghar and L. Schweitzer, J. Phys. C **14**, 5185 (1981).
[12] J. B. Boyce, M. Stutzmann, and S. E. Ready, Phys. Rev. B **32**,

6062 (1985).
[13]M. S. Conradi and R. E. Norberg, Phys. Rev. B **24**, 2285 (1981).
[14]W. E. Carlos and P. C. Taylor, Phys. Rev. B **25**, 1435 (1982).
[15]J. B. Boyce and M. Stutzmann, Phys. Rev. Lett. **54**, 562 (1985).
[16]D. J. Leopold, J. B. Boyce, P. A. Fedders, and R. E. Norberg, Phys. Rev. B **26**, 6053 (1982).
[17]D. J. Leopold, P. A. Fedders, R. E. Norberg, J. B. Boyce, and J. C. Knights, Phys. Rev. B **31**, 5642 (1985).
[18]J. A. Reimer, P. Dubois Murphy, B. C. Gerstein, and J. C. Knights, J. Chem. Phys .**74**, 1501 (1981).
[19]F. R. Jeffrey, P. Dubois Murphy, and B. C. Gerstein, Phys. Rev. B **23**, 2099 (1981).
[20]J. A. Reimer and M. A. Petrich, in *Amorphous Silicon and Related Materials, Advances in Disordered Semiconductors*, edited by H. Fritzsche (World Scientific, Singapore, 1989), Vol. 1A, pp. 3–27.
[21]B. C. Gerstein and C. R. Dybowski, *Transient Techniques in NMR of Solids* (Academic, Orlando, FL, 1985), pp. 69–78, 255–267.
[22]E. Fukushima and S. B. W. Roeder, *Experimental Pulse NMR: A Nuts and Bolts Approach* (Addison-Wesley, Reading, MA, 1981), pp. 279–282.
[23]B. C. Gerstein and C. R. Dybowski, *Transient Techniques in NMR of Solids* (Ref. 21), pp. 132–135.
[24]A. Abragam, *The Principles of Nuclear Magnetism* (Oxford University Press, New York, 1983), pp. 264–423.
[25]P. G. LeComber, A. Madan, and W. E. Spear, J. Non-Cryst. Solids **11**, 219 (1972).
[26]G. C. Levy, J. D. Cargioli, P. C. Juliano, and T. D. Mitchell, J. Am. Chem. Soc. **95**, 3445 (1973).
[27]C. P. Slichter, *Principles of Magnetic Resonance*, 3rd ed. (Springer-Verlag, New York, 1990), pp. 257–264.
[28]N. Bloembergen, Physica **15**, 386 (1949).
[29]P. G. de Gennes, J. Phys. Chem. Solids **7**, 345 (1958).
[30]W. E. Blumberg, Phys. Rev. **119**, 79 (1960).
[31]H. E. Rorschach, Jr., Physica **30**, 38 (1964).
[32]I. J. Lowe and D. Tse, Phys. Rev. **166**, 279 (1968).
[33]P. M. Henrichs, M. L. Cofield, R. H. Young, and J. M. Hewitt, J. Magn. Reson. **58**, 85 (1984).
[34]S. Hasegawa and S. Yazaki, Thin Solid Films **55**, 15 (1978).
[35]R. A. Street, D. K. Biegelsen, and J. C. Zesch, Phys. Rev. B **25**, 4334 (1982).
[36]H. C. Marsmann, W. Raml, and E. Hengge, Z. Naturforsch. Teil B **35**, 1541 (1980).
[37]E. Fukushima and S. B. W. Roeder, *Experimental Pulse NMR: A Nuts and Bolts Approach* (Ref. 22), pp. 164–176.
[38]A. H. Mahan, P. Menna, and R. Tsu, Appl. Phys. Lett. **51**, 1167 (1987).
[39]A. H. Mahan, A. Mascarenhas, D. L. Williamson, and R. S. Crandall, in *Amorphous Silicon Technology*, edited by A. Maden, M. J. Thompson, P. C. Taylor, Y. Hamakawa, and P. G. LeComber, MRS Symposia Proceedings No. 118 (Materials Research Society, Pittsburgh, 1988), p. 641.
[40]D. L. Williamson, A. H. Mahan, B. P. Nelson, and R. S. Crandall, Appl. Phys. Lett. **55**, 783 (1989).
[41]S. Hayashi, K. Hayamizu, S. Yamasaki, A. Matsuda, and K. Tanaka, Phys. Rev. B **35**, 4581 (1987).
[42]W. L. Shao, J. Shinar, B. C. Gerstein, F. Li, and J. S. Lannin, Phys. Rev. B **41**, 9491 (1990).
[43]H. Lock, R. A. Wind, G. E. Maciel, and N. Zumbulyadis, Solid State Commun. **64**, 41 (1987).
[44]M. Stutzmann and D. K. Biegelsen, Phys. Rev. B **28**, 6256 (1983).
[45]T. R. Askew, H. J. Stapleton, and K. L. Brower, Phys. Rev. B **33**, 4455 (1986).
[46]R. Orbach, Proc. R. Soc. London Ser. A **264**, 458 (1961).
[47]B. Sapoval and D. Lepine, J. Phys. Chem. Solids **27**, 115 (1966).